Biomacromol. J. Vol. 2, No. 2, 126-134, December 2016.

Biomacromolecular Journal
www.bmmj.org

Isolation and Study of S-layer Nanostructure of *Deinococcus Radiodurans* R_1

M. Abdolirad, R. Khalilzadeh* and M. Alijanianzadeh
Department of Bioscience and Biotechnology, Malek-ashtar University of Technology, Tehran, Iran
(Received 17 November 2016, Accepted 18 February 2017)

ABSTRACT

Crystalline surface layer proteins (S-layer proteins) have considerable potential for the crystalline arrays in biotechnology, biomimetics and nonlife applications, including areas such as microelectronics and molecular nanotechnology. The extensive application potential of surface layers in nanobiotechnology is according to the particular inherent attributes of the single molecular arrays consisted of uniform protein or glycoprotein subunits. Most important, functional groups on the protein lattice are arrayed in well-specified positions and orientations. Many applications of S-layers are related to the ability of isolated subunits to recrystallize into single molecular arrays in suspension, suitable surfaces or interfaces. Utilization of the s-layers as template to pattern inorganic nanostructures, requires the separation and purification of these proteins and study of their structures on solid surfaces. The hexagonally packed intermediate (Hpi) protein of *Deinococcus radiodurans* belongs to the category of S-layer proteins which form crystalline two-dimensional arrays on bacterial cell surfaces. In this study, *Deinococcus radiodurans* R_1 S-layer was purified and SDS-PAGE of purified HPI layer was analyzed by Core Laboratory Image Quantification Software. And also, secondary structure of Isolated HPI layer was evaluated by Circular Dichroism. and Zeta potential measurement was carried out to define surface charge of HPI surface layer sheets. In addition, hexagonally pattern of HPI sheets have been studied by atomic force microscopy and field emission scanning electron microscopy. According to our results, isolated HPI layer from *Deinococcus radiodurans* R_1 can be used as template to array nanoparticles in future works.

Keywords: S-layer; *Deinococcus radiodurans*; Isolation; Atomic force microscopy; Scanning electron microscopy

INTRODUCTION

The technological utilization of self-assembly systems, wherein molecules spontaneously organize into ordered structures under equilibrium, is one key challenge in nanosciences. Self-assembly systems have capability to create identical, ultrasmall functional units and the possibilities to apply such structures at macroscopic scale are reasons of their attractiveness. Utilization of crystalline cell-surface proteins (S-layer proteins) is lead to develop creative approaches for the assembly of supramolecular structures and devices with a few nanometers dimensions [1].

Surface layer (S-layer) proteins constitute the outer component of prokaryotes cell wall and are the most abundant proteins produced by cells. They are consisted of periodic repetition of the same protein (or glycoprotein) subunits with a molecular weight of 40-200 kDa depending on the particular microbial species. S-layer lattices exhibit oblique, square or hexagonal symmetries and pores with identical size and morphology in the size range of 2-8 nm. Surface layers topography and physicochemical properties are often different between inner face, which is attached to the cell, and outer face which is exposed to the external environment [1-7].

Based on the remarkable intrinsic feature of S-layers to self-assemble into two-dimensional arrays in suspension and at interfaces [8,9], they were considered by interesting applications in biotechnology and nanobiotechnology [4,5, 10-12]. However many other proteins also assemble into two-dimensional crystals[13], but there are remarkable advantages of S-layer proteins. For examples, S-layers are produced in abundance from native bacterial sources without need to genetic engineering, and they are chemical resistant. Among mentioned applications, S-layers have been used as biotemplate to pattern inorganic

*Corresponding author. E-mail: rkhalilzadeh@mut.ac.ir

nanostructures. To demonstrate the potential of S-layer proteins in biotemplating applications, S-layers from *Deinococcus radiodurans* have been used in literatures based on its chemical resistance and ease of purification in the crystalline state [14-20].

The Gram-positive bacterium, *Deinococcus radiodurans* cell envelope is composed of inner membrane, the peptidoglycan, an interstitial layer which is only known to be consisted of water soluble proteins, a lipid rich backing layer followed by the hexagonally packed intermediate S-layer (Hpi) and finally the outermost carbohydrate coat[21]. *D. radiodurans*is known to possess at least two S-layer proteins, the hexagonally packed intermediate (Hpi) protein, and SlpA (DR2577), that is homologue of an S-layer SlpA protein in *Thermus thermophiles* [22,23]. The Hpi protein consists of 1036 amino acids. The mature protein has a molecular mass of 106 kDa and a pI of 4.8. Interestingly, the Hpi protein includes seven Cys residues, which are rarely observed in S-layer proteins [24]. The secondary structure of the Hpi protein was evaluated by infrared spectroscopy: 30% of the protein is made of β-sheets/turns and the rest are random coil [25]. Transition of β-structure to random coil will be happened at low pH = 2.2. 3D reconstructions of Hpi layer up to 1.8 nm resolutions, using negatively stained, rotary-shadowed, as well as unstained, freeze-dried sample have been reported [24,26,27].

Atomic force microscopy (AFM) is a very-high-resolution apparatus for imaging topography of biomolecules at nanoscale in native and aqueous environments. The structure of Hpi have been analyzed by electron microscopy [28-30] and AFM *in vitro* [31-33] and *in vivo* [34]. AFM analyses have been demonstrated the hydrophobic inner face of the surface layer while the outerface is partly hydrophilic. In addition, AFM imaging have also been used to study the mechanical stability of molecular structure of Hpi protein at singular molecule level [31].

The isolation of Hpi layer have been done by addition of detergent to purified cell wall fragments [35,36] or whole cells [25]. The Hpi lattice displays hexagonal symmetry and exhibits a core concentrated around the six-fold axis with a reported spacing of 18 nm between each protein core region [37]. This lattice is in accordance with the hexagonally array seen on the surface of bacteria in their native state, undisturbed by sample preparation [25]. The thickness of the HPI protein layer was measured by various methods: STEM [32], STM [32], AFM [31-33] and TEM [28]. The results are variableamong 5.7 and 8.6 nm for monolayer.

Comparison of the polypeptide composition of two different strains (R_1 and Sark) of *Deinococcus radiodurans* by SDS-PAGE, have been demonstrated the absence of a prominent HPI-layer band in the vicinity of 100 kDa for strain R_1 [38]. It has been illustrated before that proteolysis happens *in vivo*, for the HPI protein layer in R_1 strain [39].

In this study, a simple method that leads to the production of high purity HPI sheets from *D. radiodurans* R_1 was used and Sodium Dodecyl Sulfate Polyacrylamide gel electrophoresis of purified Hpi layer were analyzed by CLIQS software. Furthermore, hexagonally pattern of HPI sheets have been investigated by atomic force microscopy.

METHODS

Cultivation of Microorganism

D. radiodurans R_1 was obtained as lyophilized culture from Iranian Biological and genetic Resource National Center and transferred to 5 ml growth media (1% Tryptone, 0.5% glucose, 0.5% yeast extract, 0.5% NaCl). It was grown overnight in incubator-shaker at 30 °C and plated onto media solidified with 1.5% agar. Single bacteria colonies were cultured at 30 °C overnight in the proper growth media. Glycerol was added to 30% (vol/vol) final concentration and 5 ml stock was stored at -80 °C. For cultivation, a small amount of frozen cells were transferred to 20 ml of freshly prepared growth media and cells were grown overnight at 30 °C in incubator-shaker. The overnight culture was utilized to inoculate 1 l of growth media and cells were grown at 30 °C under agitation (180 rpm). Growth was traced by evaluating the optical density of the solution at 600 nm. Cells were harvested at early stationary phase by centrifugation at 7000 × *g* for 10 min and washed two times by resuspension in deionized water, followed by centrifugation as above.

S-layer Protein Purification

HPI sheets were purified *via* differential centrifugation. Cells were stripped of their S-layers by incubation in 2wt% lithium dodecyl sulfate (LDS) for 4 h at 4 °C. The

suspension was centrifuged at low speed of 3000 *g* for 15 min to remove denuded cells, and the supernatant was transferred to fresh centrifuge tubes. S-layer proteins were sedimented by centrifugation at 20000 *g* for 30 min. To obtain HPI-layer sheets free of any associated proteins, pelleted proteins were subjected to a further detergent incubation (2% SDS, 60 °C, 30 min); the HPI layer was sedimented via centrifugation at 20000 *g* for 30 min. The HPI sheets washed 3 times in 1 ml of DI water by repeated resuspension-centrifugation at 20000 *g* as above. The HPI layer stock solution (~0.5 mg ml^{-1} protein in ultrapure de-ionized water) was stored at 4 °C until further use.

S-layer proteins concentration was calculated based on the Bradford assay using bovine serum albumin (BSA) as the standard [40].

SDS gel electrophoresis. SDS-PAGE electrophoresis was exploited to define the molecular mass of S-layer subunits. Therefore, isolated subunits were applied into a 12% gel [40]. HPI sheets samples (0.5 mg ml^{-1}) were detached in the sample buffer by heating and incubation them at 100 °C for 2 min. The sample load per slot and electrophoresis at a constant voltage of 90V was terminated when the bromophenol blue dye reached the bottom of the slab (4 h). Gels were stained with Coomassie Brilliant Blue dye and destained with destaining solution following standard procedures. The following markers were used: beta-galactosidase (116 kDa), bovine serum albumin (66.2 kDa), ovalbumin (45.0 kDa), lactate dehydrogenase (35.0 kDa), REase Bsp98I (25.0 kDa), beta-lactoglobulin (18.4 kDa), lysozyme (14.4 kDa).

Core laboratory image quantification software (CLIQS). CLIQS, Totallab Ltd. will compute protein size based on a lane with standard markers. Totallab's Core Laboratory Image Quantification Software (CLIQS) suggests a variety of functions to analyze gels. It can automatically detect lanes and bands, estimate molecular weights according to a standard.

Evaluation of Secondary Structure of Isolated HPI Layer by Circular Dichroism (CD)

As respects, common conformational motifs such as α-helixes, β-sheets and turns which have different specification in Far-UV CD spectra, investigation of secondary structure of HPI layer after isolation was done by Circular Dichroism (CD) spectroscopic technique. CD measurements were performed using AVIV 215 Spectropolarimeter (AVIV, USA) at 25 °C. Far- UV spectra (190-260 nm) were recorded in a continuous mode. Bandwidth of 1 nm was used. The HPI layer concentration of 0.35 mg ml^{-1} was prepared in Dionized water and protein absorbance spectrum were plotted as ellipticity versus wavelength. Secondary structure content was estimated by Deconvolution CDNN software (version 2.1).

Zeta Potential Measurements of HPL Layer

The zeta potential measurements of Isolated HPI layer were carried out using Zetasizer Nano instruments (Malvern Instruments, Worcestershire, UK).

Atomic Force Microscopy

Atomic force microscope (AFM) (ARA-AFM, manufactured by Ara-Research Company in Iran, Tehran) in tapping mode, equipped with NSC36/Al BS silicon tips (with an aluminum coating on the cantilever backside; Mikro Masch company) was used for the topographic (height) imaging of samples. AFM Images were analyzed by Imager version 1.00 Ara-Research Company.

HPI sheets were diluted to a concentration of 50 µg ml^{-1} and a 50 µl drop of HPI solution adsorbed onto freshly cleaved mica for 1 h and subsequently rinsed by several separate drops of DI H_2O (30 s each wash) then allowed to be dried by air.

Electron Microscopy

Field emission scanning electron microscopy (FE-SEM) (MIRA3 TESCAN, Razi Foundation, Iran) was used to confirm hexagonally structure of isolated HPI layer. Prior to SEM imaging, an ultrathin layer of gold (<2 nm) was sputtered onto S-layer samples. SEM image was obtained at low accelerating voltage to minimize damage to the organic structure on the surface.

RESULTS AND DISCUSSION

Figure 1 presents the growth curve of *D. radiodurans.* Growth curve reveals the transition from the exponential phase of growth (where cells grow at their maximum possible rate) to the stationary phase, at which point all

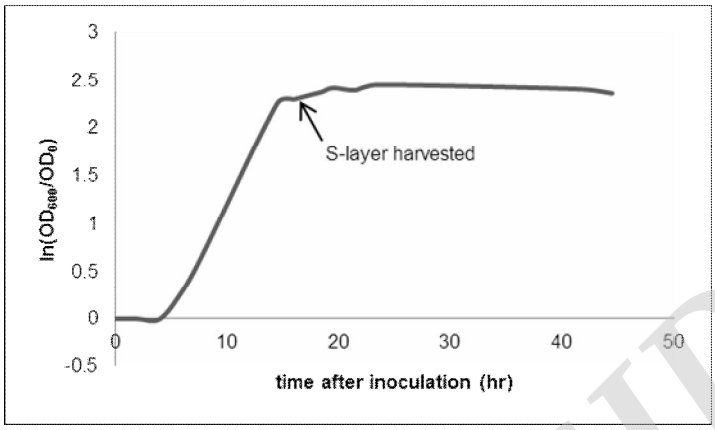

Fig. 1. Growth curve of *Deinococcus radiodurans* R_1. Growth was monitored by measuring the optical density of the solution at λ = 600 nm.

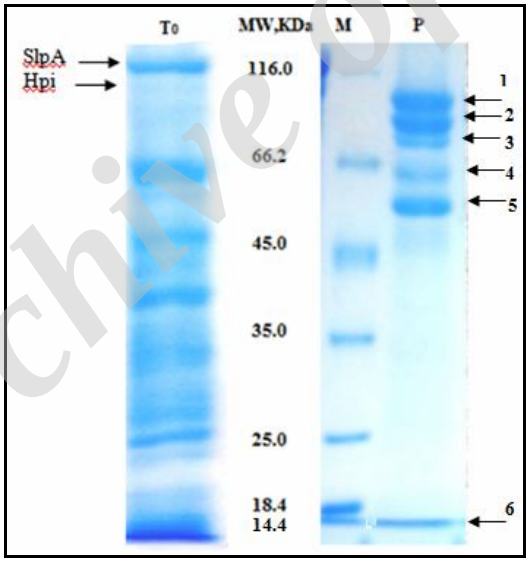

Fig. 2. SDS-polyacrylamide gel electrophoresis analysis of HPI layer from *Deinococus radiodurans* R_1. T_0: *Deinococus radiodurans* R_1 polypeptide composition, M: Marker molecular weight, P: HPI protein after SDS treatment (60 °C, 30 min). Arrows indicate S-layer proteins in lane T_0 and purified HPI layer in lane P.

nutrients in a culture have been used up and there is not any net cell growth. To maximize the recovery yield of surface layer proteins, the optimum time to collect is in early stationary phase.

After cells have been collected, the next step is to purify S-layers. Suspension of *D. radiodurans* cells, in lithium dodecyl sulfate (LDS) at low temperature (4 °C) causes large crystalline patches of S-layer proteins and interstitial materials released to the medium. Denuded cells can be separated from materials in suspension and S-layer proteins

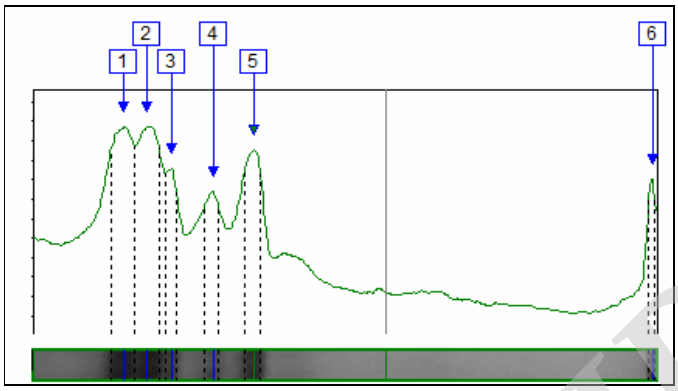

Fig. 3. SDS-PAGE analyzed by CLIQS software. The peaks show bands which are detected by software. (Molecular weights: 1 = 100 kDa, 2 = 91 kDa, 3 = 84 kDa, 4 = 61 kDa, 5 = 53 kDa, 6 = 14 kDa).

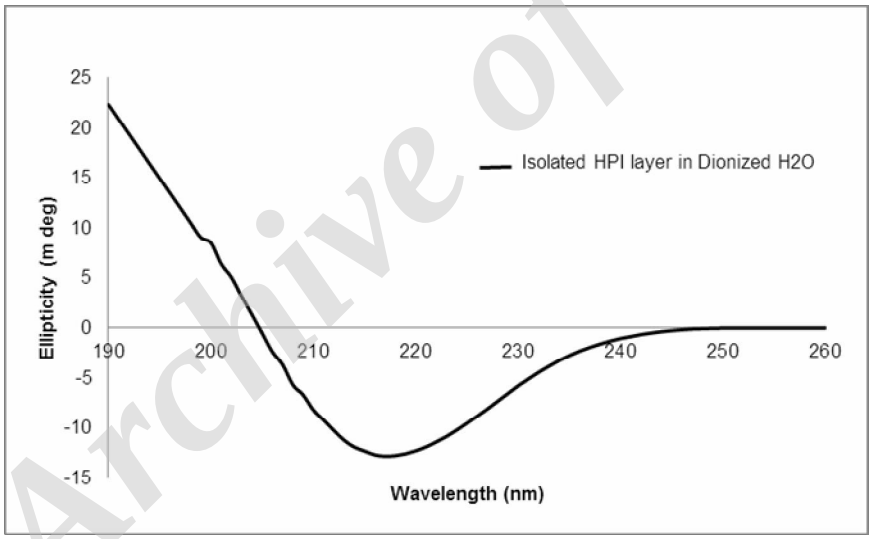

Fig. 4. Far-UV CD spectra of HPI layer of *Deinococcus radiodurans* at 25 °C: Fresh HPI layer in Dionized H_2O.

can be purified from other proteins by differential centrifugation. Gel electrophoresis prepares evidence to confirm the purity of the isolated S-layers.

Figure 2 shows polypeptide composition of *Deinococus radiodurans* $R_1$by SDS-polyacrylamide gel electrophoresis. As described, S-layer of *D. radiodurans* is specified by a regular repetition of pores believed to be consisted of only one protein called the HPI with about 106 KDa and SlpA with about 123 KDa. As regards, S-layer proteins are the dominant protein of cell, the sharpest band in high molecular weight is about 123 KDa, which is related to SlpA and because of proteolysis of HPI *in vivo*, no sharp band about 100 KDa has been observed and also there isn't any sharp band in high molecular weight. These results have been corresponded with previous studies [38,39].

To disappear 123 KDa polypeptide in isolated protein, product of differential centrifuge was treated by sodium dodecyl sulfate (SDS) at 60 °C for 30 min (Fig. 2, lane P).

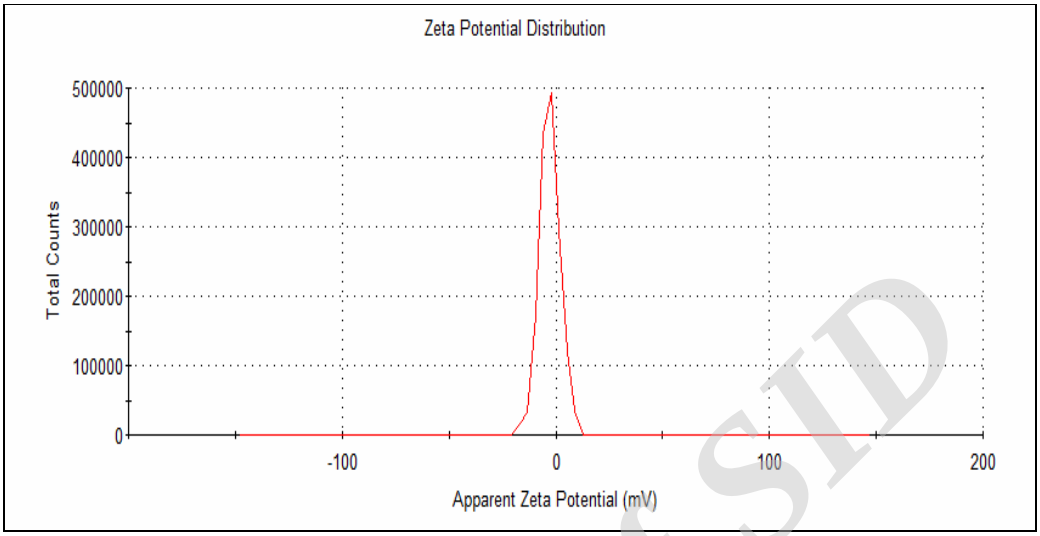

Fig. 5. Zeta potential measurements of isolated HPI layer.

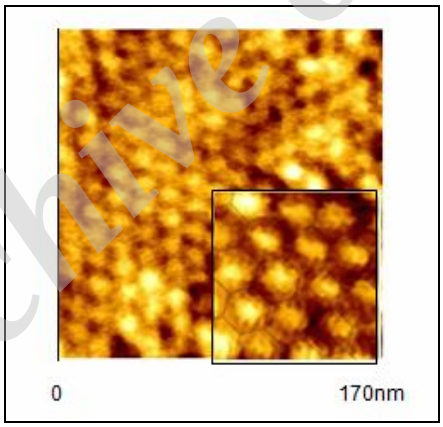

Fig. 6. AFM image of Hexagonally pattern of HPI layer.

Lane P was analyzed by Core Laboratory Image Quantification Software (CLIQS) and the molecular weights of bands were approximately calculated (Fig. 3). Six bands were detected by software and molecular weights were calculated 100, 91, 84, 61, 53 and 14 kDa respectively which are near the molecular weights of these bands in previous works but the number of weak bands in our work were fewer than previous works [21]. As mentioned, these weak bands are because of proteolysis of HPI layer *in vivo* and it doesn't affect the structure of HPI layer [39]. Furthermore, the percentage of bands were achieved 26.26%, 27.56%, 10.53%, 14.02%, 16% and 5%, respectively by CLIQS software.

In order to specify secondary structure of HPI layer after isolation, Far-UV CD spectra was taken in the region of 190-260 nm at 25 °C by using AVIV 215 spectropolarimeter. Far-UV CD spectra of HPI layer has been shown in Fig. 4. According to CDNN analysis, secondary structure of HPI layer is consisted of β-sheets

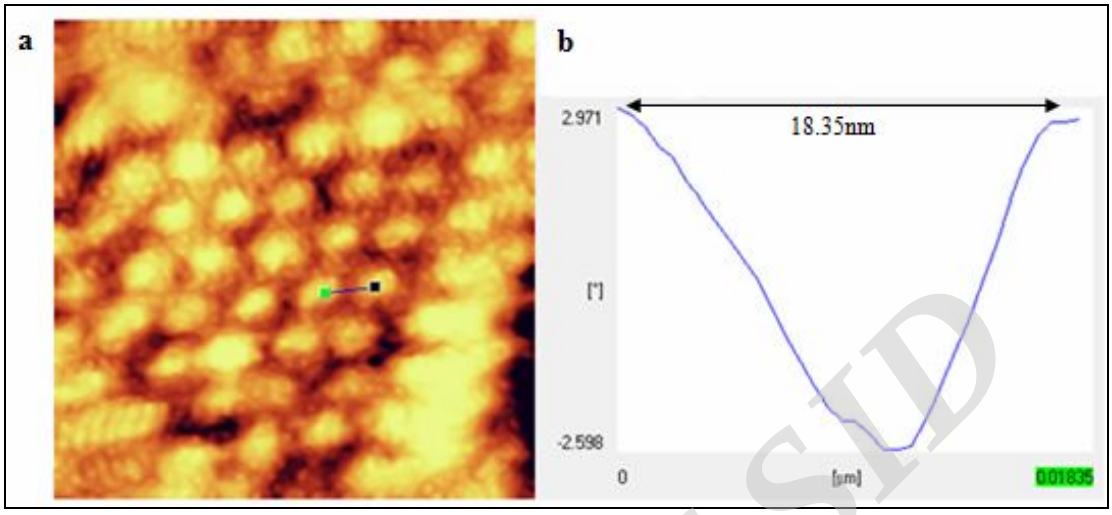

Fig. 7. Determination of lattice constant of HPI layer inner face. (a) AFM height image of HPI S-layer. (b)Section analysis profile across the area marked by the green square in the height image in (a).

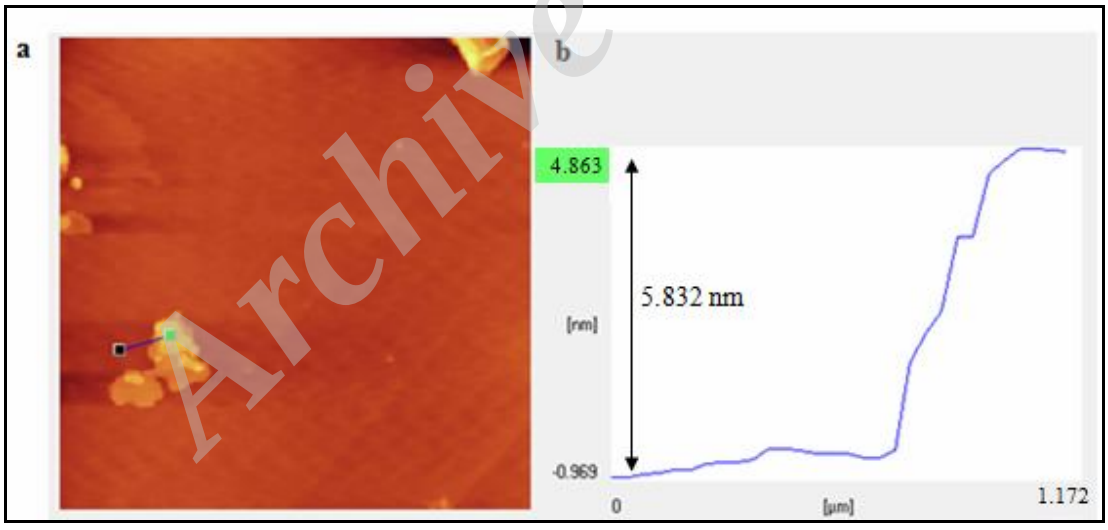

Fig. 8. Determination of monolayer thickness of HPI S-layers by Atomic force microscopy (AFM). (a) AFM height image of HPI S-layer (10 µm × 10 µm scan area). (b) Section analysis profile across the area

37%, β-turns 20%, random coil 46% and Alpha helix 17%. The sum of the secondary structure elements is upper than 100% with 20% deviation which it can be because of that reference spectra is not suitable for handling our data. Before that Baumeister *et al*. [25] estimated secondary structure of HPI layer by Infrared spectroscopy, in which HPI layer contained 30% of β-structure and the rest random coil.

As previously stated, charge distribution and surface

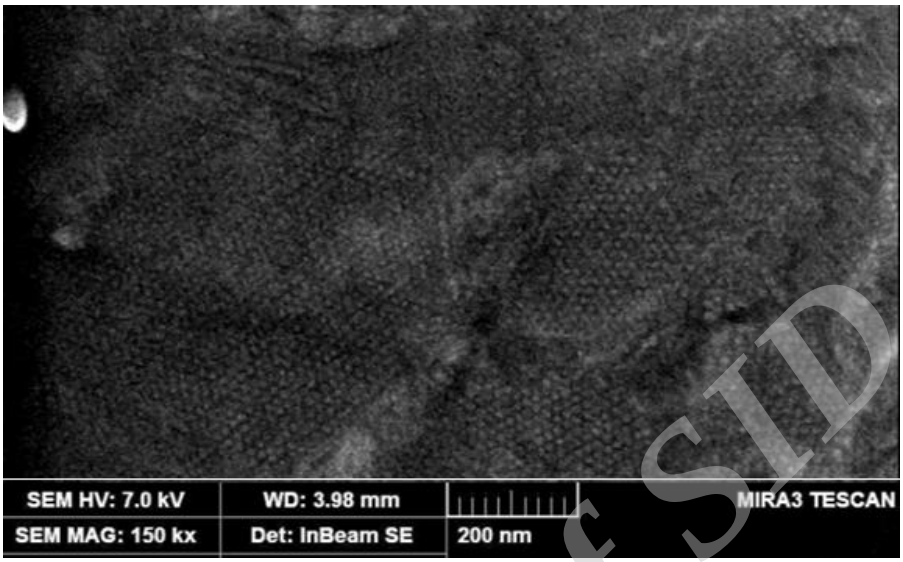

Fig. 9. FE-SEM image of hexagonally structure of HPI S-layers.

topography of the S-layer self-assembly structures are different between two sides. Inner face of HPI layer is hydrophobic and outer face of HPI layer is hydrophilic with net negative or positive charges. The zeta potential of HPI layer was found as a sharp peak at -2.82 mV (Fig. 5), which it is suggested that outer face of HPI layer has net negative charge. Before that, net negative charge of hydrophilic side of Bacillus surface layer was determined [6].

Primary analyses to confirm the lattice dimensions and integrity of the purified HPI sheet fragments were performed by using tapping mode AFM. Surface layer proteins could be observed on solid surfaces by AFM. AFM examination of HPI layers have been done on mica. Figure 6 illustrates the expected hexamer structure of HPI layer, which indicates that HPI layer remains its morphology lattice after purification procedure. Of course, there is another view that this hexagonally structure is related to band 1 in lane P which exists in an uncleaved state and its molecular weight near to molecular weight of mature HPI.
So maybe, 26.26% of purified HPI keep their hexagonal structure.

From analyses of AFM images, the lattice constant of HPI was determined in this work to be 18.35 nm (Fig. 7).

As shown in Fig. 8, AFM (topographical height) imaging of the S-layer fragments on freshly cleaved mica revealed that the HPI protein monolayer is ~6 nm thick. It was concluded that the correct thickness is around 8 nm [32] which alters by different methods. One of the reasons of this difference is air-drying of HPI layer. Hexagonally structure of HPI layer was also confirmed by FE-SEM analysis which has been exhibited in Fig. 9.

CONCLUSIONS

Deinococcus radiodurans R_1 S-layer proteins was isolated by LDS and its purity analyzed by SDS-PAGE. The molecular weights and percentage of S-layer subunits were calculated by CLIQS software. Six bands with molecular weights of 100, 91, 84, 61, 53 and 14 kDa were detected. Approximately, secondary structure of HPI layer contains 37% of β-sheets, 20% of β-turns, 46% of random coil and 17% of Alpha helix. And outer face of HPI surface layer has net negative charge according to zeta potential measurement. The HPI layer have been studied by tapping mode of atomic force microscopy and hexagonally pattern of HPI layer have been observed. AFM analysis in this study revealed that HPI protein monolayer is ~6 nm and its lattice constant is 18.35 nm which are consistent with theoretical values. In addition, hexagonally structure of HPI surface layer sheets confirmed by field emission scanning electron microscopy. According to microscopy images,

isolated HPI layer from *Deinococcus radiodurans* R_1 can be used as template to array nanoparticles in future works.

ACKNOWLEDGEMENTS

We appreciate Ara-Research Company for using AFM.

REFERENCES

[1] E. Egelseer, N. Ilk, D. Pum, P. Messner, C. Schaffer, B. Schuster,U.B. Sleytr, in: M.C. Flickinger (Eds.), Encyclopedia of Industrial Biotechnology: Bioprocess, Bioseparation, and Cell Technology, John Wiley & Sons, Hoboken, 2009.
[2] U.B. Sleytr, B. Schuster, E.M. Egelseer, D. Pum, FEMS Microbiol. Rev. (2014) 1.
[3] P. Messner, C. Schaffer, E. Egelseer, U.B. Sleytr, in: H. Konig, H. Claus, A. Varma (Eds.), Prokaryotic Cell Wall Compounds, Springer, Berlin, 2010.
[4] V. Debabov, Mol. Biol. 38 (2004) 482.
[5] U.B. Sleytr, B. Schuster, D. Pum, IEEE Eng. Med. Biol. Mag. (2003) 140.
[6] M. Sara, U.B. Sleytr, J. Bacteriol. 182 (2000) 859.
[7] G. Babolmorad, G. Emtiazi, R. Emamzadeh, Appl. Biochem. Biotechnol. 173 (2014) 103.
[8] F. Baneyx, J.F. Matthaei, Curr. Opin. Biotechnol. 28 (2014) 39.
[9] D. Pum, J. Toca-Herrera, U.B. Sleytr, Int. J. Mol. Sci.. 14 (2013) 248.
[10] N. Ilk, E.M. Egelseer, U.B. Sleytr, Curr. Opin. Biotechnol. 22 (2011) 824.
[11] D. Pum, U. Sleytr, Trends. Biotechnol. 17 (1999) 8.
[12] U. Sleytr, M. Sara, P. Messner, D. Pum, Ann. N. Y. Acad. Sci. 745 (1994) 261.
[13] B.K. Jap, M. Zulauf, T. Scheybani, A. Hefti, W. Baumeister, U. Aebi,A. Engel, Ultramicroscopy. 46 (1992) 45.
[14] Y. Sierra-Sastre, S.A. Dayeh, S.T. Picraux, C.A. Batt, ACS Nano. 4 (2010) 1209.
[15] Y. Sierra-Sastre, S. Choi, S.T. Picraux, C.A. Batt, J. Am. Chem. Soc. 130 (2008) 10488.
[16] S.S. Marka, M. Bergkvist, P. Bhatnagar, C. Welch, A.L. Goodyear, X. Yang, E.R. Angert, C.A. Batt, Colloids Surf. B 57 (2007) 161.
[17] S.S. Mark, M. Bergkvist, X. Yang, L.M. Teixeira, P. Bhatnagar, E.R. Angert, C.A. Batt, Langmuir. 22 (2006) 3763.
[18] D.B. Allred, M. Sarikaya, F. Baneyx, D.T. Schwartz, Nano Lett. 5 (2005) 609.
[19] E. Gyorvary, A. Schroedter, D. Talapin, H. Weller, D. Pum, U. Sleytr, J. Nanosci. Nanotechnol. 4 (2004) 115.
[20] D.B. Allred, M. Sarikaya, F. Baneyx, D.T. Schwartz, Electrochim. Acta 53 (2007) 193.
[21] C.S. Misra, B. Basu, S.K. Apte, Biochim. Biophys. Acta 1848 (2015) 3181.
[22] H. Rothfuss, J.C. Lara, A.K. Schmid, M.E. Lidstrom, Microbiol. 152 (2006) 2779.
[23] D. Farci, M.W. Bowler, J. Kirkpatrick, S. Mcsweeney, E. Tramontano, D. Piano, Biochim. Biophys. Acta 1838 (2014) 1978.
[24] S. Howorka, Progress in Molecular Biology and Translational Science, Academic Press, 2011.
[25] W. Baumeister, F. Karrenberg, R. Rachel, A. Engel, B.T. Heggeler, W.O. Saxton, Eur. J. Biochem. 125 (1982) 535.
[26] W. Saxton, W. Baumeister, J. Microsc. 127 (1982) 127.
[27] W. Baumeister, O. Kubler, H.P. Zingsheim, J. Ultrastruct. Res. 75 (1981) 60.
[28] W. Baumeistert, M. Barth, R. Hegerl, R. Guckenberger, M. Hahn, W. Saxton, J. Mol. Biol. 187 (1986) 241.
[29] W. Baumeister, O. Koblert, Proc. Natl. Acad. Sci. U.S.A. 75 (1978) 5525.
[30] E. Work, H. Griffiths, J. Bacteriol. 95 (1968) 641.
[31] D.J. Muller, W. Baumeister, A. Engel, Proc. Natl. Acad. Sci. U.S.A. 96 (1999) 13170.
[32] D.J. Muller, W. Baumeister, A. Engel, J. Bacteriol. 178 (1996) 3025.
[33] S. Karrasch, R. Hegerl, J.H. Hoh, W. Baumeister, A. Engel, Proc. Natl. Acad. Sci. U.S.A. 91 (1994) 836.
[34] T.E. Lister, P.J. Pinhero, Langmuir 17 (2001) 2624.
[35] B.G. Thompson, R.G.E. Murray, J.F. Boyce, Can. J. Microbiol. 28 (1982) 1081.
[36] P. Lancy, R.G.E. Murray, Can. J. Microbiol. 14 (1978) 162.
[37] D.J. Muller, W. Baumeister, A. Engel, J. Bacteriol. 178 (1996) 3025.
[38] F.H. Karrenberg, I. Wildhaber, W. Baumeister, Curr. Microbiol. 16 (1987) 15.
[39] R. Rachel, A. Engel, W. Baumeister, FEMS Microbiol. Lett. 17 (1983) 115.
[40] J.M. Walker, ed. The Protein Protocols Handbook, Humana Press, New Jersey, 2002.